land

MDPI

Article

Analysis of the Spatial–Temporal Characteristics of Vegetation Cover Changes in the Loess Plateau from 1995 to 2020

Zhihong Yao [1], Yichao Huang [1], Yiwen Zhang [1], Qinke Yang [2,*], Peng Jiao [3,*] and Menghao Yang [1]

[1] College of Surveying and Geo-Informatics, North China University of Water Resources and Electric Power, Zhengzhou 450046, China; yaozhihong@ncwu.edu.cn (Z.Y.); hycchao@163.com (Y.H.); zywwww29@163.com (Y.Z.); yangmenghao@ncwu.edu.cn (M.Y.)
[2] Department of Urban and Resource Sciences, Northwest University, Xi'an 710069, China
[3] Yellow River Institute of Hydraulic Research, Zhengzhou 450003, China
* Correspondence: qkyang@nwu.edu.cn (Q.Y.); hnzzjp2010@126.com (P.J.)

Abstract: The Loess Plateau is one of the most severely affected regions by soil erosion in the world, with a fragile ecological environment. Vegetation plays a key role in the region's ecological restoration and protection. This study employs the Geographical Detector (Geodetector) model to quantitatively assess the impact of natural and human factors, such as temperature, precipitation, soil type, and land use, on vegetation growth. It aims to reveal the characteristics and driving mechanisms of vegetation cover changes on the Loess Plateau over the past 26 years. The results indicate that from 1995 to 2020, the vegetation coverage on the Loess Plateau shows an increasing trend, with a fitted slope of 0.01021 and an R^2 of 0.96466. The Geodetector indicates that the factors with the greatest impact on vegetation cover in the Loess Plateau are temperature, precipitation, soil type, and land use. The highest average vegetation coverage is achieved when the temperature is between −4.8 and 2 °C or 12 and 16 °C, precipitation is between 630.64 and 935.51 mm, the soil type is leaching soil, and the land use type is forest. And the interaction between all factors has a greater effect on the vegetation cover than any single factor alone. This study reveals the factors influencing vegetation growth on the Loess Plateau, as well as their types and ranges, providing a scientific basis and guidance for improving vegetation coverage in this region.

Keywords: Loess Plateau; NDVI; vegetation cover; land use; geographical detector model

Academic Editor: Elias Symeonakis

Received: 27 December 2024
Revised: 22 January 2025
Accepted: 29 January 2025
Published: 1 February 2025

Citation: Yao, Z.; Huang, Y.; Zhang, Y.; Yang, Q.; Jiao, P.; Yang, M. Analysis of the Spatial–Temporal Characteristics of Vegetation Cover Changes in the Loess Plateau from 1995 to 2020. *Land* **2025**, *14*, 303. https://doi.org/10.3390/land14020303

1. Introduction

Vegetation is a vital element of the Earth's ecosystem [1] and plays a crucial role in influencing soil erosion on the Loess Plateau [2]. In semi-arid environments, the distribution pattern of vegetation is a major driving force and a preventive measure against soil erosion [3]. Fractional vegetation cover (FVC) represents the proportion of the ground area covered by the vertical projection of vegetation, including leaves, stems, and branches, relative to the total area of a given region. It is a widely used parameter for evaluating the relationship between vegetation and soil erosion [4], often used to reflect ecological and environmental issues and, to some extent, assess changes in the region's ecological environment [5–9]. The Normalized Difference Vegetation Index (NDVI), due to its spectral sensitivity to green plants, is often used in studies of vegetation conditions [10–12]. Studies have proven that the NDVI can accurately estimate vegetation cover [4,13]. Many researchers now use pixel binary models with NDVI to estimate the vegetation cover [14–16], while others use pixel ternary models for estimation [17,18].

The Loess Plateau is located in the middle reaches of the Yellow River and serves as a critical ecological barrier for the Yellow River Basin. However, the region has long suffered from severe soil erosion [19]. Vegetation restoration and ecological rehabilitation can significantly enhance regional climate regulation, reduce the frequency of sandstorms, improve ecosystem stability, and support the sustainable economic and social development of the Yellow River Basin. To address the increasingly severe soil erosion on the Loess Plateau, China has implemented various projects since the late 1990s, such as the "Grain-for-Green" program, to mitigate soil erosion and improve land quality [20–22]. Vegetation plays a crucial role in controlling soil erosion on the Loess Plateau, and changes in vegetation coverage to some extent reflect the status of soil and water loss in the region. Therefore, studying vegetation cover changes on the Loess Plateau provides valuable guidance for ecological restoration efforts.

The factors influencing changes in vegetation cover include natural and human factors. Among natural factors, climate has a particularly significant impact on vegetation cover changes. Studies have shown a strong correlation between vegetation cover changes and temperature and precipitation [23,24]. Different soil types exhibit notable differences in supporting vegetation growth, and existing research indicates that soil variables affect vegetation structure and species diversity [25]. Other natural factors, such as topographical features, also influence vegetation formation and coverage, with the slope gradient and aspect affecting regional vegetation moisture, solar radiation, and temperature [26,27]. Human factors, likewise, play a crucial role in vegetation cover changes. For instance, land use changes are considered the most direct and comprehensive indicator of human activities and are the primary drivers of long-term vegetation changes in China [28,29]. Additionally, some scholars have analyzed the effects of human activities such as population growth [30], urbanization, economic development levels, over-cultivation, overgrazing, and ecological protection policies on vegetation cover changes [31]. Considering these factors comprehensively, this study selects temperature, precipitation, soil type, elevation, slope gradient, and slope aspect as natural factors, while the land use type, population density, and GDP are chosen as human factors.

Earlier studies mostly employed linear, trend, and correlation analysis methods to qualitatively analyze the spatiotemporal changes in vegetation cover [32,33], but were unable to quantitatively evaluate the influencing factors. With the advent of the Geographical Detector model [34,35], an increasing number of researchers have adopted it to quantitatively assess the factors influencing vegetation cover [36–38]. The Geographical Detector is a spatial analysis model designed to detect spatial heterogeneity and reveal the driving forces behind it. This statistical method overcomes the limitations of traditional mathematical statistical models, such as large parameter requirements, numerous assumptions, and isolated factor analysis [39], while exploring the interaction between explanatory factors and the analyzed variables. Vegetation cover changes on the Loess Plateau are influenced by multiple factors. The Geographical Detector enables an integrated analysis of these factors, revealing their impact on vegetation cover through different detectors that assess the response of vegetation cover to single and multiple factors [40].

This study aims to quantitatively assess the impact of various factors on vegetation cover changes in the region, identify the types or ranges of factors conducive to vegetation growth, and provide scientific guidance for improving vegetation coverage on the Loess Plateau.

2. Materials and Methods

2.1. Study Area

The Loess Plateau is located in the central–northern part of China (100–114° E, 33–41° N), primarily encompassing parts of seven provinces: Shaanxi, Gansu, Ningxia, Qinghai, Shanxi, Inner Mongolia, and Henan (Figure 1). The total area of the loess region on the Loess Plateau is 635,000 km^2, making it one of the most severely affected regions by soil erosion in the world. The topography of the Loess Plateau descends from the higher northwest to the lower southeast, with mountains, hills, and plateaus being the primary landform type. The Loess Plateau experiences a typical temperate continental monsoon climate, marked by cold, dry winters and hot, rainy summers, along with considerable temperature fluctuations between day and night. The multi-year average temperature on the Loess Plateau ranges from −13 °C to 16 °C, showing a three-tiered distribution with a strong spatial pattern. As shown in Figure 2a, the southern and eastern regions of the Loess Plateau have the highest average temperatures, followed by the central and northern regions, while the western region has the lowest average temperatures. Influenced by monsoon circulation, the multi-year average precipitation on the Loess Plateau decreases progressively from approximately 700 mm in the southeast to around 100 mm in the northwest (Figure 2b). The main land use types on the Loess Plateau include forest, grassland, and cropland, with grassland being the most extensive. The primary soil types are incipient soil, semi-lateritic soil, caliche soil, and arid soil, with incipient soil covering the largest area, accounting for nearly half of the Loess Plateau.

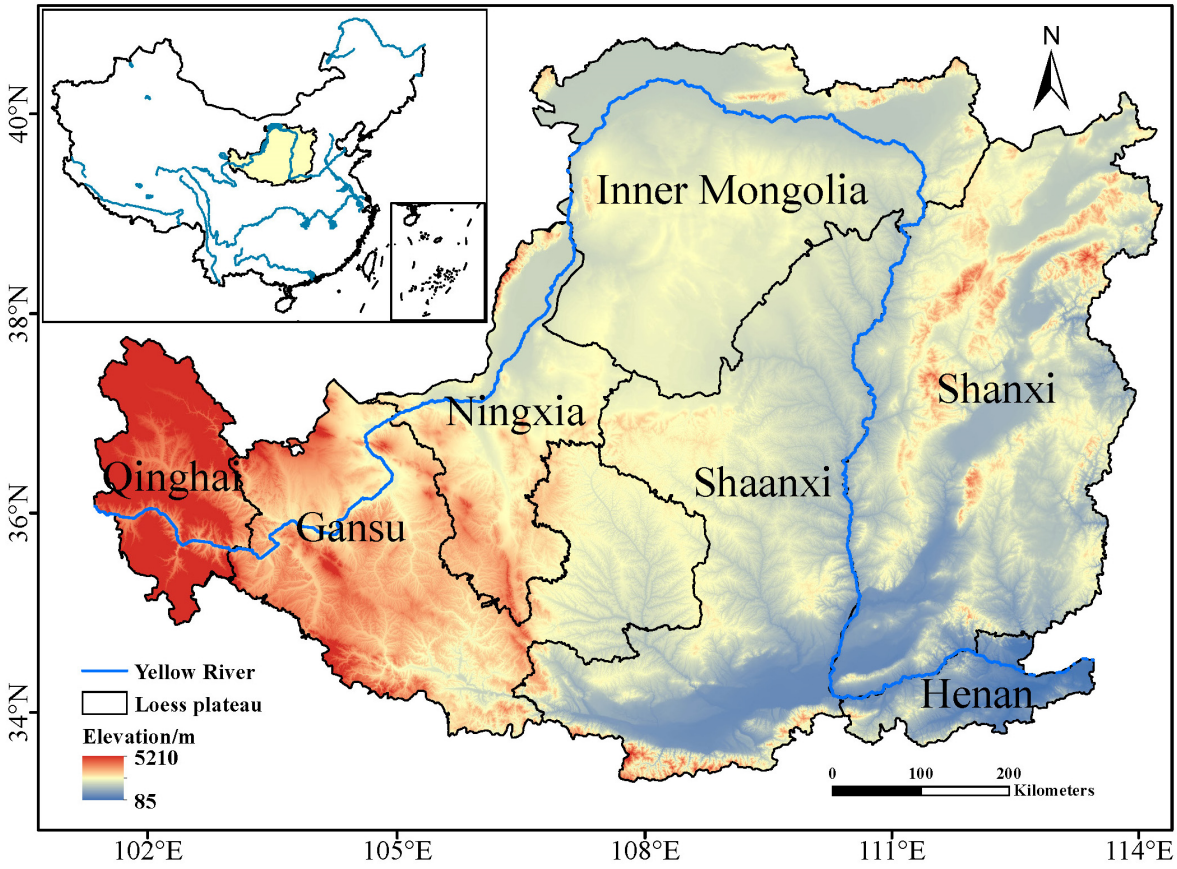

Figure 1. Map of the Loess Plateau geographic location.

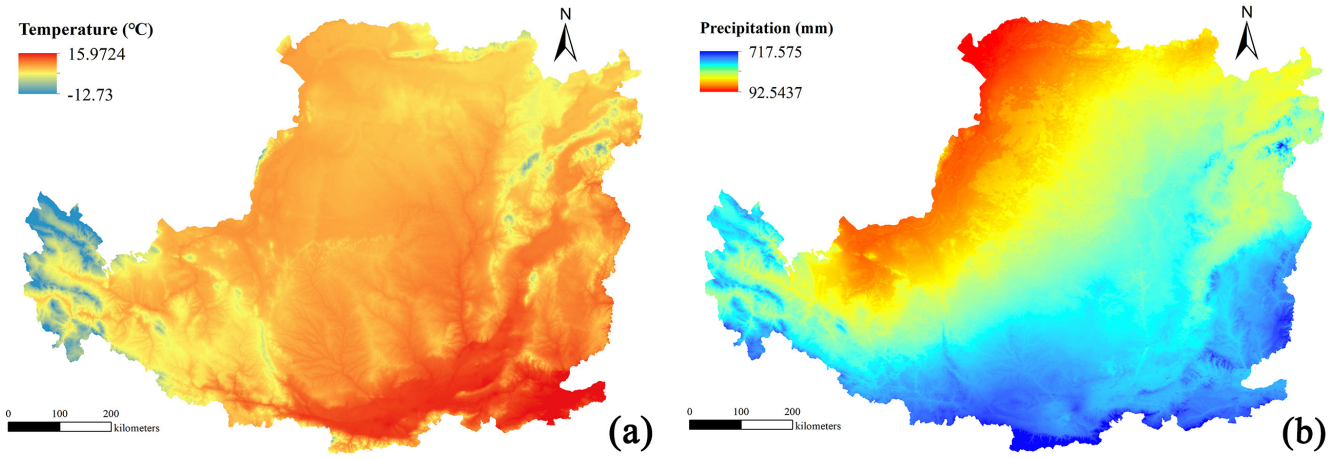

Figure 2. The long−term average precipitation and temperature values of the Loess Plateau: (**a**) temperature; (**b**) precipitation.

2.2. Data Sources

NDVI data were derived from the GIMMS NDVI dataset (1995–2015) and the MODIS NDVI dataset (2001–2020). The GIMMS NDVI13g dataset, developed by NASA, has a spatial resolution of 8 km and a temporal resolution of 15 days. The MOD13A1 dataset features a spatial resolution of 500 m and a temporal resolution of 16 days. To construct a long-term dataset suitable for this study, two NDVI datasets were resampled to achieve a unified spatial resolution, followed by maximum value compositing to generate monthly NDVI datasets. The resampling method used was Bicubic Interpolation. Considering that the Geographical Detector requires all data to have consistent spatial resolution, the NDVI data were resampled to a 1 km resolution. For the overlapping period from 2001 to 2015, the average NDVI for each of the 12 months was calculated separately for both datasets, as shown in Figure 3. During this 15-year period, the annual average NDVI difference between the two datasets was only 0.008, indicating that the GIMMS NDVI data from 1995 to 2000 can serve as a complementary dataset to MODIS NDVI on an interannual scale.

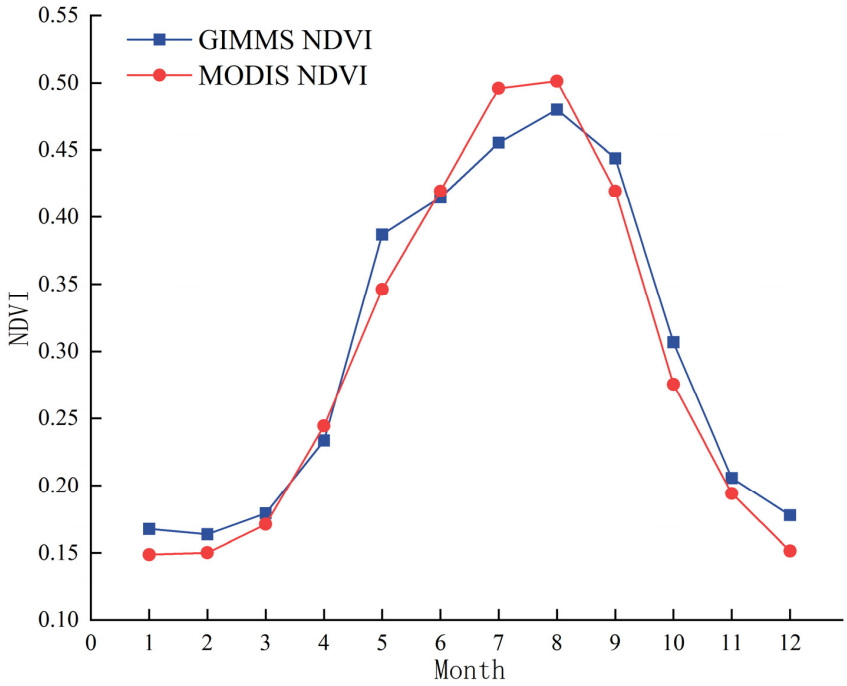

Figure 3. Monthly average NDVI from 2001 to 2015.

The elevation data were derived from ASTER GDEM, obtained from the Geospatial Data Cloud platform of the Computer Network Information Center, Chinese Academy of Sciences (http://www.gscloud.cn/, accessed on 20 December 2024), with a spatial resolution of 30 m. After mosaicking and clipping, the digital elevation data for the Loess Plateau was generated. Slope and aspect data (Figure 4a,b) were calculated from the elevation data of the Loess Plateau using ArcGISdesktop 10.8, with a spatial resolution of 30 m.

Meteorological data were supplied by the National Tibetan Plateau/Third Pole Environment Data Center (http://data.tpdc.ac.cn/, accessed on 20 December 2024), featuring a spatial resolution of 1 km and covering the period from January 1995 to December 2020. The dataset was generated for China using data from CRU and WorldClim, following the Delta spatial downscaling scheme. Temperature and precipitation data were spatially interpolated using the Thin Plate Spline (TPS) and Kriging interpolation methods. Projection coordinate transformations were applied to the results to obtain monthly and annual meteorological raster data corresponding to the NDVI data [41,42]. Figure 4c,d show the temperature and precipitation data for the Loess Plateau in 2020, respectively.

The soil type data were obtained from the Scientific Data Registration and Publishing System of the Geographic Remote Sensing Ecological Network (www.gisrs.cn/, accessed on 20 December 2024), with a spatial resolution of 30 m, as shown in Figure 4e. This dataset was digitized based on the Soil Map of the People's Republic of China, compiled and published by the National Soil Survey Office. The original data are reliable and verified through extensive field surveys and ground sampling.

Land use data were sourced from the National Glacier, Frozen Soil, and Desert Scientific Data Center (http://www.ncdc.ac.cn/, accessed on 20 December 2024), with a spatial resolution of 30 m. The land use data are part of China's first annual Landsat-derived land cover product (CLCD) from 1995 to 2020, developed by Yang Jie and Huang Xin from Wuhan University [43]. This product was constructed using 335,709 Landsat images from the Google Earth Engine platform. Training samples were collected by combining stable samples extracted from the Chinese Land Use/Cover Dataset (CLUD) with visually interpreted samples from satellite time series data, Google Earth, and Google Maps. Multiple temporal indicators were created using all available Landsat data and fed into a Random Forest classifier to generate classification results. For this study, the land use data were categorized into six land use types based on the land use classification standards: cultivated land, forest, grassland, water bodies, construction land, and unused land [44]. The land use for the Loess Plateau in 2020 is shown in Figure 4f.

The GDP and population density data were obtained from the Resource and Environment Science and Data Center of the Chinese Academy of Sciences (https://www.resdc.cn/, accessed on 20 December 2024), with a spatial resolution of 1 km, and covering the period from 1995 to December 2020 (Figure 4g,h). The GDP spatial distribution dataset was generated based on county-level GDP statistics. It incorporates spatial interaction patterns between GDP and factors closely related to human activities, such as land use types, nighttime light intensity, and residential density, through spatial interpolation to produce a gridded dataset. The multi-year average GDP of the study area is 5.11×10^6 CNY/km^2. The population density dataset was derived from county-level population statistics. It integrates multiple factors closely associated with population distribution, such as land use types, nighttime light intensity, and residential density. Using a multi-factor weight allocation method, the population data, initially based on administrative units, was distributed onto a spatial grid to achieve spatial representation of population density. The multi-year average population density of the study area is 152.672 persons/km^2.

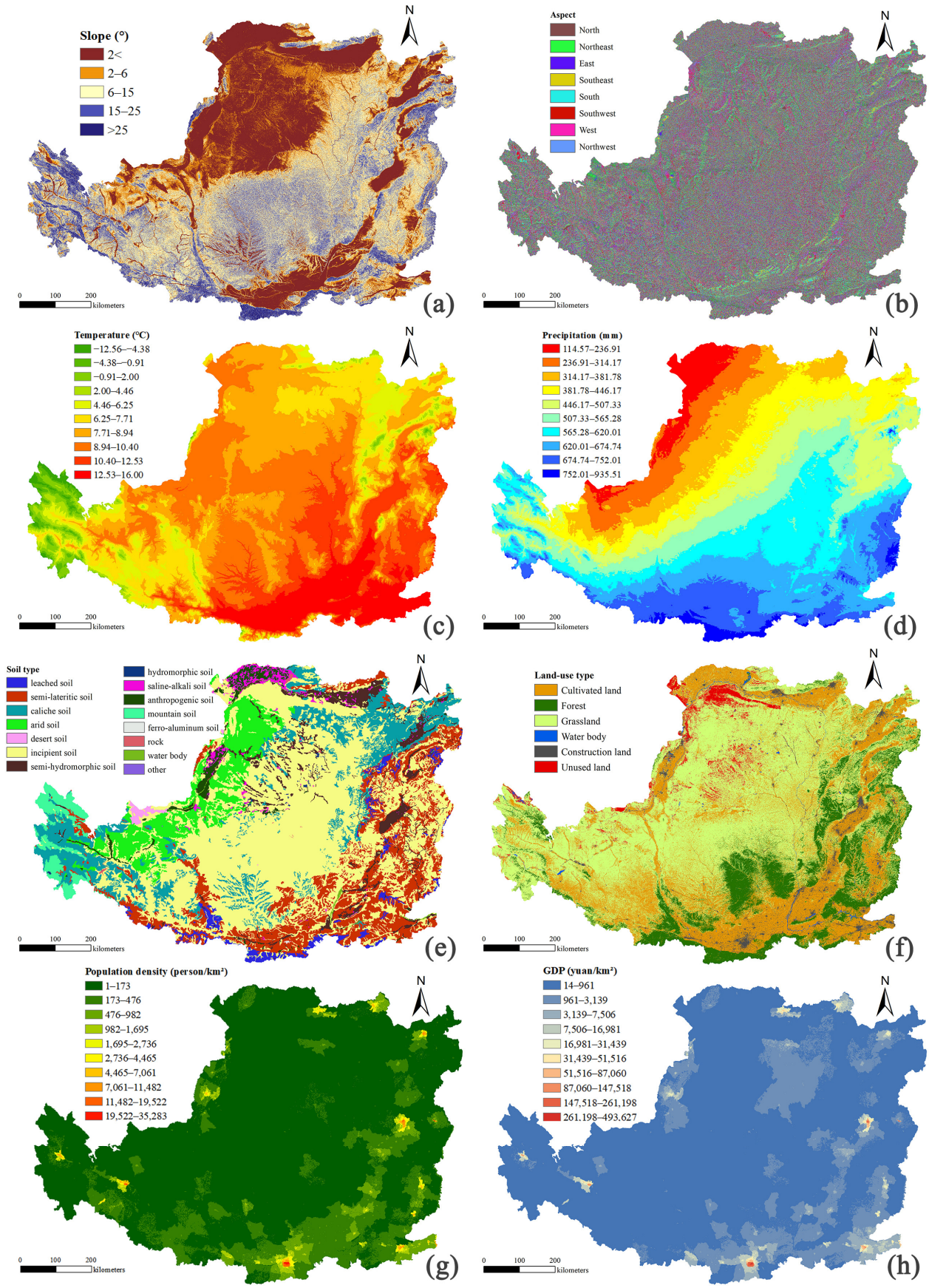

Figure 4. Spatial distributions of natural and human factors in 2020: (**a**) slope; (**b**) aspect; (**c**) temperature; (**d**) precipitation; (**e**) soil type; (**f**) land use type; (**g**) population density; and (**h**) GDP.

2.3. Method

2.3.1. Pixel Binary Mode

In remote sensing estimation methods for vegetation cover, the pixel dichotomy model is one of the more commonly used approaches. This model assumes that the surface of a pixel consists of both vegetated and non-vegetated areas, and the proportion of the vegetated area within the pixel represents the fractional vegetation cover (FVC) for that pixel. By establishing a conversion relationship between the Normalized Difference Vegetation Index (NDVI) and FVC, the vegetation cover information within the pixel can be extracted. Finally, the FVC for each pixel is calculated to determine the vegetation cover across the entire study area. The formula for calculating FVC is as follows:

$$\mathrm{FVC} = (\mathrm{NDVI} - \mathrm{NDVI_{soil}}) / (\mathrm{NDVI_{veg}} - \mathrm{NDVI_{soil}}) \quad (1)$$

where FVC represents the fractional vegetation cover, $\mathrm{NDVI_{soil}}$ refers to the NDVI value of pixels in non-vegetated or bare soil areas, and $\mathrm{NDVI_{veg}}$ denotes the NDVI value of pixels fully covered by vegetation. To eliminate the influence of outliers in NDVI values, this study selects the 5% to 95% range of cumulative pixel percentages as the confidence interval. That is, $\mathrm{NDVI_{soil}}$ corresponds to the NDVI value at the 5th percentile of the cumulative pixel percentage, while $\mathrm{NDVI_{veg}}$ corresponds to the NDVI value at the 95th percentile of the cumulative pixel percentage.

2.3.2. Theil–Sen Median

The Theil–Sen Median method, also referred to as Sen's slope estimator, is a robust non-parametric statistical technique for calculating trends. It is computationally efficient, resistant to measurement errors and outliers, and well suited for analyzing trends in long-term time series data [45]. The calculation formula is as follows:

$$\rho = Median\left(\frac{X_j - X_i}{j - i}\right) \quad 1 < i < j < n \quad (2)$$

In the formula, n represents the number of study years, X_i and X_j are the FVC values for the ith and jth years, respectively, and ρ represents the trend. When $\rho < 0$, it indicates that the FVC is showing a downward trend over time; when $\rho > 0$, it indicates that the FVC is showing an upward trend over time.

2.3.3. Mann–Kendall

The Mann–Kendall test is a non-parametric technique used to evaluate trends in time series data. It does not require the data to adhere to a normal distribution and remains unaffected by missing values and outliers, making it ideal for testing significant trends in lengthy time series datasets. The Mann–Kendall test can only identify monotonic trends and cannot detect volatility or complex non-monotonic changes in the data. If the trend exhibits cyclical variations, the MK test may not accurately reflect it. In this study, although the interannual mean of the FVC on the Loess Plateau exhibits some volatility, the overall trend is monotonic upward, so the MK test can be applied. In this study, the MK values for the vegetation cover time series on the Loess Plateau from 1995 to 2020 were calculated on a pixel-by-pixel basis and visualized.

The calculation formula for the test is as follows:

$$Z = \begin{cases} \frac{S-1}{\sqrt{Var(S)}}, S > 0 \\ 0, S = 0 \\ \frac{S+1}{\sqrt{Var(S)}}, S < 0 \end{cases} \quad (3)$$

where

$$S = \sum_{i=1}^{n-1} \sum_{j=i+1}^{n} \operatorname{sgn}(x_j - x_i) \tag{4}$$

$$\operatorname{sgn}(x_j - x_i) = \begin{cases} 1, x_j - x_i > 0 \\ 0, x_j - x_i = 0 \\ -1, x_j - x_i < 0 \end{cases} \tag{5}$$

$$Var(S) = \frac{n(n-1)(2n+5)}{12} \tag{6}$$

In the formula, S and Z are statistical test statistics, and $x = x_1, x_2, \ldots, x_n$ represents the sequence, where n is the number of data points in the sequence, and the rejection region is $\left\{|Z| > Z_{1-\frac{a}{2}}\right\}$. This means that when the value of $|Z|$ exceeds 1.65, 1.96, and 2.58, it demonstrates that the vegetation trend has successfully passed significance tests at confidence levels of 90%, 95%, and 99%, respectively.

The combination of Theil–Sen Median trend analysis and Mann–Kendall significance testing demonstrates a good effect in assessing trend changes in long time series data, and it is widely used in vegetation analysis [46]. Table 1 describes the types of trends corresponding to different experimental results.

Table 1. Mann–Kendall test trend categories.

ρ		Z	Trend Features
$\rho > 0$	{	$2.58 < Z$	Extremely significant upward trend
		$1.65 < Z < 2.58$	Significant upward trend
		$1.65 > Z$	No significant trend
$\rho = 0$		Z	No significant trend
$\rho < 0$	{	$2.58 < Z$	No significant trend
		$1.65 < Z < 2.58$	Significant downward trend
		$1.65 > Z$	Extremely significant downward trend

2.3.4. Geographical Detector Model

This study utilizes the Geographical Detector model to investigate the driving mechanisms behind vegetation cover changes on the Loess Plateau. The principle of geographical detector is shown in Figure 5. This model consists of four components: factor detection, interaction detection, risk detection, and ecological detection. In line with the objectives of this study, the factor detector, risk detector, and interaction detector were selected for use.

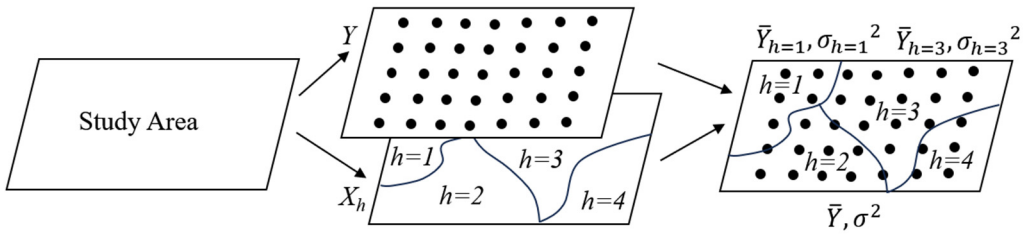

Figure 5. The principle of geographical detector.

(1) Factor detector: Factor detection is employed to assess the degree to which each factor accounts for the spatial differentiation of vegetation cover changes on the Loess Plateau. The calculation formula is as follows:

$$q = 1 - \frac{\sum_{h=1}^{L} Nh\sigma_h^2}{N\sigma^2} \tag{7}$$

In the formula, the value of q ranges from (0, 1). The magnitude of the q value indicates the explanatory power of the factor regarding spatial changes in vegetation cover; a higher value signifies a stronger influence of that factor on the spatial variation of vegetation cover. $h = 1, \ldots, L$ represents the stratification of various natural and anthropogenic factors X, as shown in Table 2. σ^2 is the overall variance of vegetation cover, while ${\sigma_h}^2$ represents the variance of vegetation cover corresponding to the stratification h. For convenience, in the study, all factors were resampled to a spatial resolution of 1 km.

Table 2. Classification of natural and human factors.

Natural Factors	Human Factors
Elevation (x_1)	Land use (x_7)
Slope (x_2)	Population density (x_8)
Aspect (x_3)	GDP (x_9)
Temperature (x_4)	
Precipitation (x_5)	
Soil types (x_6)	

(2) Risk detection: Risk detection involves calculating the average vegetation cover for a particular influencing factor across different sub-regions, followed by statistical analysis and significance testing of the results. Based on the average values and their significance, the suitable growth range for vegetation is determined. Regions with higher FVC mean values are considered suitable for vegetation growth.

(3) Interaction Detection: Interaction detection is used to identify whether the combined effects of two different factors enhance or weaken their influence on the spatial differentiation of the dependent variable. $q(x_1)$ and $q(x_2)$ represent the q values of the two different factors affecting vegetation cover. By comparing the interaction effect with the sum of $q(x_1)$, $q(x_2)$, and $q(x_1 \cap x_2)$, we can determine whether the interaction of factors x_1 and x_2 promotes or suppresses vegetation cover. The specific comparison method is shown in Table 3.

Table 3. Types of two-factor interactions.

Discriminant Criteria	Types of Interactions
$q(x_1 \cap x_2) < Min(q(x_1), q(x_2))$	weaken, nonlinear
$Min(q(x_1), q(x_2)) < q(x_1 \cap x_2) < Max(q(x_1), q(x_2))$	single factor weaken, nonlinear
$q(x_1 \cap x_2) > Max(q(x_1), q(x_2))$	dual-factor enhancement
$q(x_1 \cap x_2) = q(x_1) + q(x_2)$	dual-factor independent
$q(x_1 \cap x_2) > q(x_1) + q(x_2)$	enhance, nonlinear

3. Results

3.1. Temporal and Spatial Changes in Vegetation Coverage

3.1.1. Temporal Changes

Figure 6 shows the interannual average vegetation coverage on the Loess Plateau from 1995 to 2020. As illustrated, the interannual average vegetation coverage increased from 0.36 to 0.6 over the 26 years. Although there were minor fluctuations, the overall trend was a monotonic increase, with a fitted slope of 0.1021.

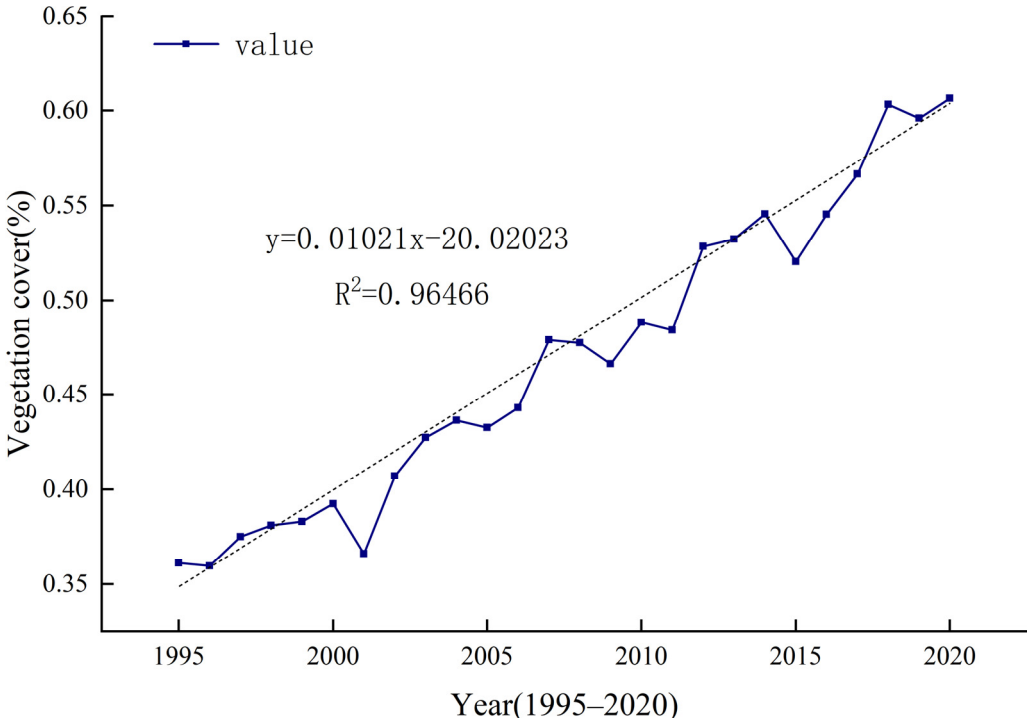

Figure 6. Annual mean FVC changes in the Loess Plateau from 1995 to 2020.

3.1.2. Spatial Differentiation

Figure 7 shows the distribution of vegetation coverage change trends on the Loess Plateau from 1995 to 2020, with 1995 as the baseline year. As shown, over the past 26 years, the vegetation cover in most areas of the Loess Plateau has demonstrated a highly significant upward trend, while a small number of areas show a significant upward trend. Some regions exhibit no obvious trend, primarily consisting of established forested land. A very small portion of the area has shown a significant or highly significant downward trend due to the increase in construction land.

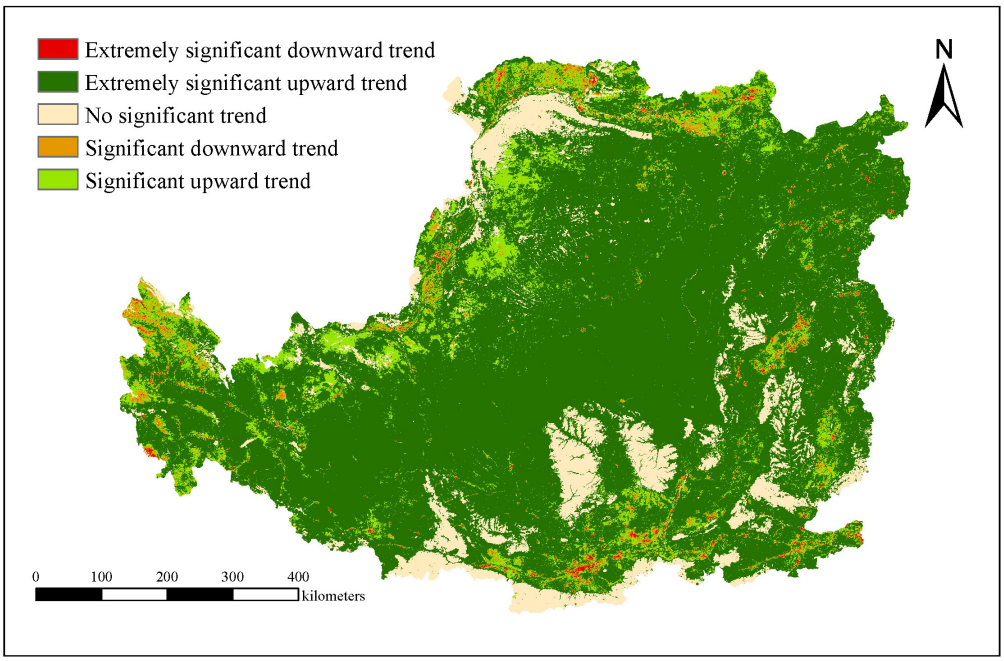

Figure 7. Trend of vegetation coverage change from 1995 to 2020, using the Mann–Kendall test.

3.2. Analysis of the Driving Factors of Vegetation Cover Changes

3.2.1. Factor Detection

The factor detector calculates the q values to investigate the extent to which each factor influences vegetation cover. Among the various factors, the p values serve as significance tests for the q values, all of which are less than 0.05, indicating that the q values of both natural and anthropogenic factors have statistical significance. Table 4 presents the q values of each factor for the years 1995, 2000, 2010, and 2020. Notably, the q values for temperature, precipitation, soil type, and land use are all greater than 0.2, indicating that these factors are the primary driving elements with the most significant impact on the spatial changes in vegetation cover on the Loess Plateau.

Table 4. The explanatory power of various factors on FVC in 1995, 2000, 2010, and 2020.

Factors	*q* Values			
	1995	**2000**	**2010**	**2020**
Elevation	0.114	0.113	0.11	0.095
Slope	0.133	0.135	0.152	0.201
Aspect	0.001	0.001	0.001	0.001
Temperature	0.251	0.241	0.245	0.231
Precipitation	0.394	0.641	0.657	0.682
Soil types	0.354	0.352	0.35	0.336
Land use	0.459	0.465	0.468	0.418
Population density	0.014	0.014	0.009	0.006
GDP	0.1	0.079	0.019	0.013

From the analysis of the explanatory power of multiple factors on vegetation cover changes during different research periods (Table 4), it can be observed that in 1995, land use type had the greatest impact on vegetation cover. During this period, policies such as returning farmland to forest and afforestation were implemented, resulting in significant changes in land use on the Loess Plateau, with some farmland and grassland being converted into forest land. Temperature and precipitation were the most significant natural factors affecting vegetation cover in 2000, 2010, and 2020. Interestingly, in 1995, in addition to land use type, temperature and precipitation emerged as the key influential factors, highlighting their critical role in vegetation growth. The soil type maintained a stable and relatively high level of influence on vegetation cover across all four time periods, underscoring its significant impact on vegetation cover. In contrast, factors such as elevation, slope, aspect, GDP, and population density had relatively minor influences on vegetation cover and thus are not considered important influencing factors.

3.2.2. Risk Detection

Precipitation is a key factor affecting vegetation growth. With the continuous increase in precipitation, vegetation cover also shows an increasing trend. Using the natural breaks method in ArcGIS, precipitation was divided into 10 intervals, represented by numbers 1 to 10. The percentage of area occupied by each interval was then calculated, as shown in Table 5. Figure 8 presents the average FVC for different precipitation intervals. It can be seen from the figure that within the precipitation range of 300–900 mm, the average FVC values at the four time points show a monotonic increasing trend. Moreover, in most precipitation intervals, the average FVC values increase year by year over time. The results indicate that from the second interval onward, there is a positive correlation between precipitation and the average FVC. Within the valid data range, higher precipitation corresponds to better vegetation growth conditions.

Table 5. Percentage of area occupied by each precipitation zone.

Zone Code	1995		2000		2010		2020	
	Zone	Percentage	Zone	Percentage	Zone	Percentage	Zone	Percentage
1	90.66–209.38	6.48%	106.52–196.60	6.29%	107.81–226.01	8.42%	114.57–236.91	4.43%
2	209.38–285.23	7.63%	196.60–259.39	8.08%	226.01–298.75	8.95%	236.91–314.17	7.25%
3	285.23–351.18	10.60%	259.39–322.18	10.92%	298.75–359.37	10.95%	314.17–381.78	9.92%
4	351.18–413.84	22.48%	322.18–379.50	13.34%	359.37–416.96	14.12%	381.78–446.17	12.10%
5	413.84–476.49	17.79%	379.50–428.64	17.30%	416.96–471.51	12.55%	446.17–507.33	13.46%
6	476.49–535.85	14.66%	428.64–475.04	13.37%	471.51–523.04	13.86%	507.33–565.28	12.66%
7	535.85–591.92	11.21%	475.04–524.18	11.78%	523.04–571.53	12.22%	565.28–620.01	15.50%
8	591.92–651.27	5.96%	524.18–570.58	10.39%	571.53–623.05	10.96%	620.01–674.74	13.42%
9	651.27–733.72	3.00%	570.58–630.64	6.63%	623.05–698.83	6.86%	674.74–752.01	9.56%
10	733.72–931.58	0.18%	630.64–802.62	1.90%	698.83–880.68	1.10%	752.01–935.51	1.71%

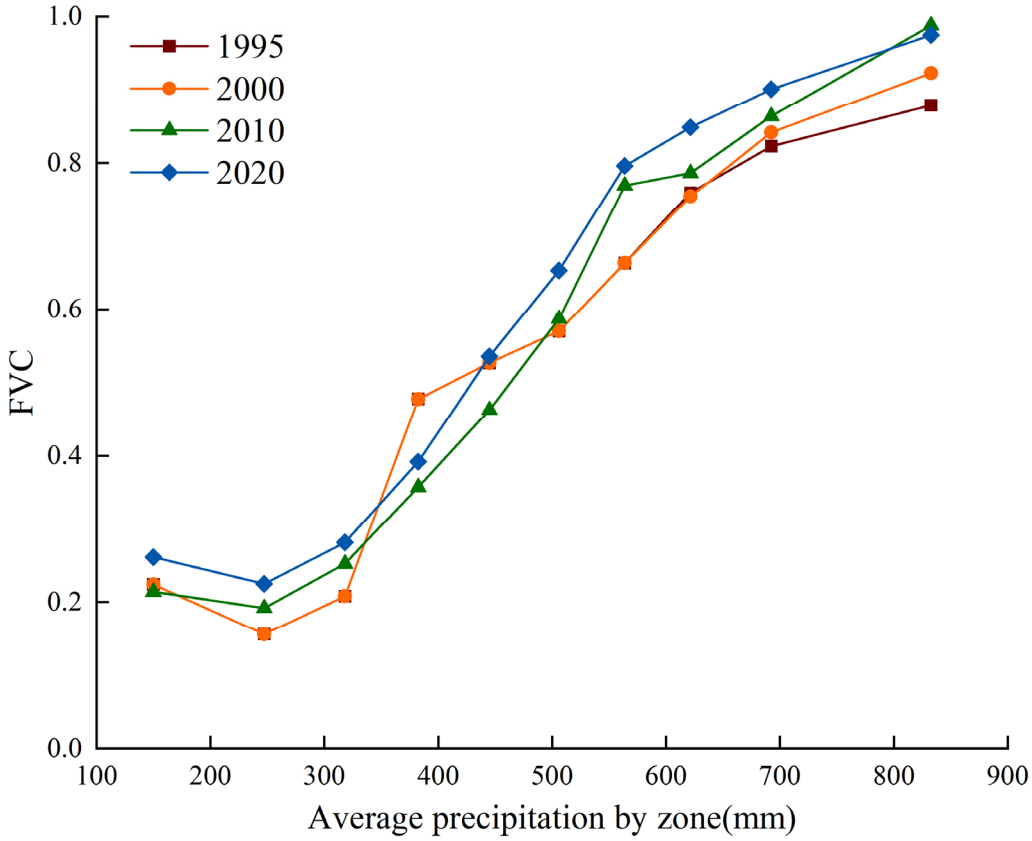

Figure 8. Average FVC value for each precipitation zone in 1995, 2000, 2010, and 2020.

Temperature has a direct impact on the photosynthesis, respiration, and transpiration of vegetation. Extreme temperatures, whether too low or too high, affect the growth and developmental physiological processes of plants. Using the natural breaks method, temperature was divided into 10 intervals, represented by numbers 1 to 10, and the percentage of area occupied by each interval was calculated (Table 6). Figure 9 shows the average FVC for different temperature intervals. As shown in the figure, the line graphs at the four time points all exhibit an N-shaped pattern, indicating that within the temperature range of this study, FVC first increases, then decreases, and finally increases again with temperature. In most intervals, the average FVC corresponding to the same temperature increases over time. It is worth noting that the FVC averages for each year exhibit two peaks in the 2nd and 3rd intervals and the 9th and 10th intervals. In this study, the maximum average FVC value occurs at the first peak. However, at the second peak, the average FVC still shows a positive correlation with temperature. Given that the average temperature on the Loess Plateau is rising year by year, it is possible that, in the foreseeable future, as the temperature

on the plateau increases further, the maximum average FVC value may shift to a position to the right of the second peak.

Table 6. Percentage of area occupied by each temperature zone.

Zone Code	1995		2000		2010		2020	
	Zone	Percentage	Zone	Percentage	Zone	Percentage	Zone	Percentage
1	−13.20–−5.19	0.49%	−13.11–−4.91	0.49%	−12.67–−4.55	0.49%	−12.56–−4.38	0.49%
2	−5.19–−1.75	1.06%	−4.91–−1.42	1.06%	−4.55–−1.05	1.05%	−4.38–−0.91	1.05%
3	−1.75–1.02	1.66%	−1.42–1.49	1.65%	−1.05–1.87	1.64%	−4.38–2.00	1.64%
4	1.02–3.36	2.30%	1.49–3.96	2.34%	1.87–4.35	2.32%	2.00–4.46	2.31%
5	3.36–5.18	6.05%	3.96–5.65	6.90%	4.35–6.15	6.74%	4.46–6.25	6.78%
6	5.18–6.58	12.52%	5.65–6.99	13.45%	6.15–7.62	14.69%	6.25–7.71	14.49%
7	6.58–7.80	22.96%	6.99–8.34	24.84%	7.62–8.86	23.92%	7.71–8.94	24.40%
8	7.80–9.25	28.74%	8.34–9.80	27.40%	8.86–10.32	27.44%	8.94–10.40	27.66%
9	9.25–11.47	14.56%	9.80–12.05	12.77%	10.32–12.58	12.62%	10.40–12.53	11.99%
10	11.47–15.14	9.66%	12.05–15.53	9.09%	12.58–16.07	9.08%	12.53–16.00	9.18%

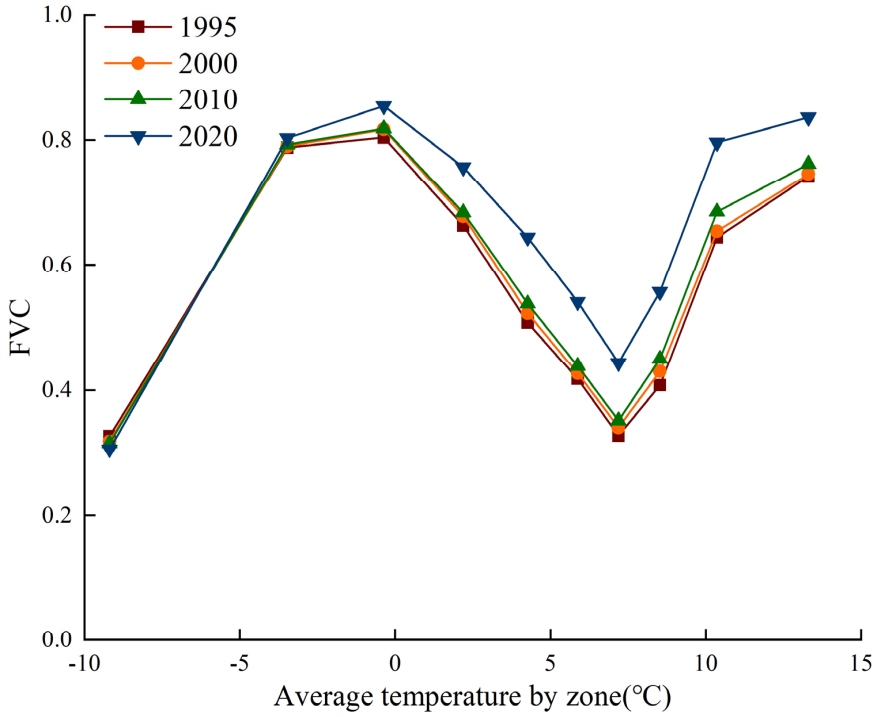

Figure 9. Average FVC value for each temperature zone in 1995, 2000, 2010, and 2020.

Under different soil types, significant differences in the average vegetation cover are observed due to variations in the soil moisture content and organic matter content. The soils in the study area were divided into 15 categories, each represented by a corresponding number, and the percentage of area occupied by each soil type was calculated (Table 7). Figure 10 shows the average FVC for different soil types in 1995, 2000, 2010, and 2020. It can be observed that for most soil types, the average FVC value increases over time, with a significant rise in 2020 compared to the other years. The results indicate that leached soil, semi-leached soil, and alpine soil have a favorable promoting effect on vegetation growth.

Land use was classified into six categories, represented by numbers 1 to 6, and the percentage of area occupied by each category was calculated (Table 8). Figure 11 shows the average FVC for different land use types across different years; it can be seen from the figure that the average FVC in 2020 is significantly higher than in other years. This is because, during the study period, the average FVC of the Loess Plateau reached its peak in 2020. It can be noted that the average vegetation cover for unused land is the lowest, remaining below 0.2. In contrast, forest land corresponds to the largest vegetation cover area, with an average above 0.9 during the study period. It is worth noting that the average

FVC value of construction land in the study area is higher than that of grassland, which is an uncommon phenomenon. However, considering that most of the grassland in the study area is located in the arid northwest with relatively low precipitation, vegetation growth is relatively poor, and vegetation cover is present only for a limited period within a year. As a result, the annual average FVC is lower than that of construction land.

Table 7. Percentage of area occupied by each soil type.

Zone Code	Soil Type	Percentage
1	leached soil	2.17%
2	semi-lateritic soil	15.41%
3	caliche soil	13.25%
4	arid soil	8.58%
5	desert soil	0.39%
6	incipient soil	48.86%
7	semi-hydromorphic soil	5.15%
8	hydromorphic soil	0.11%
9	saline–alkali soil	1.36%
10	anthropogenic soil	1.68%
11	mountain soil	2.54%
12	ferro-aluminum soil	0.03%
13	rock	0.15%
14	water body	0.31%
15	other	0.01%

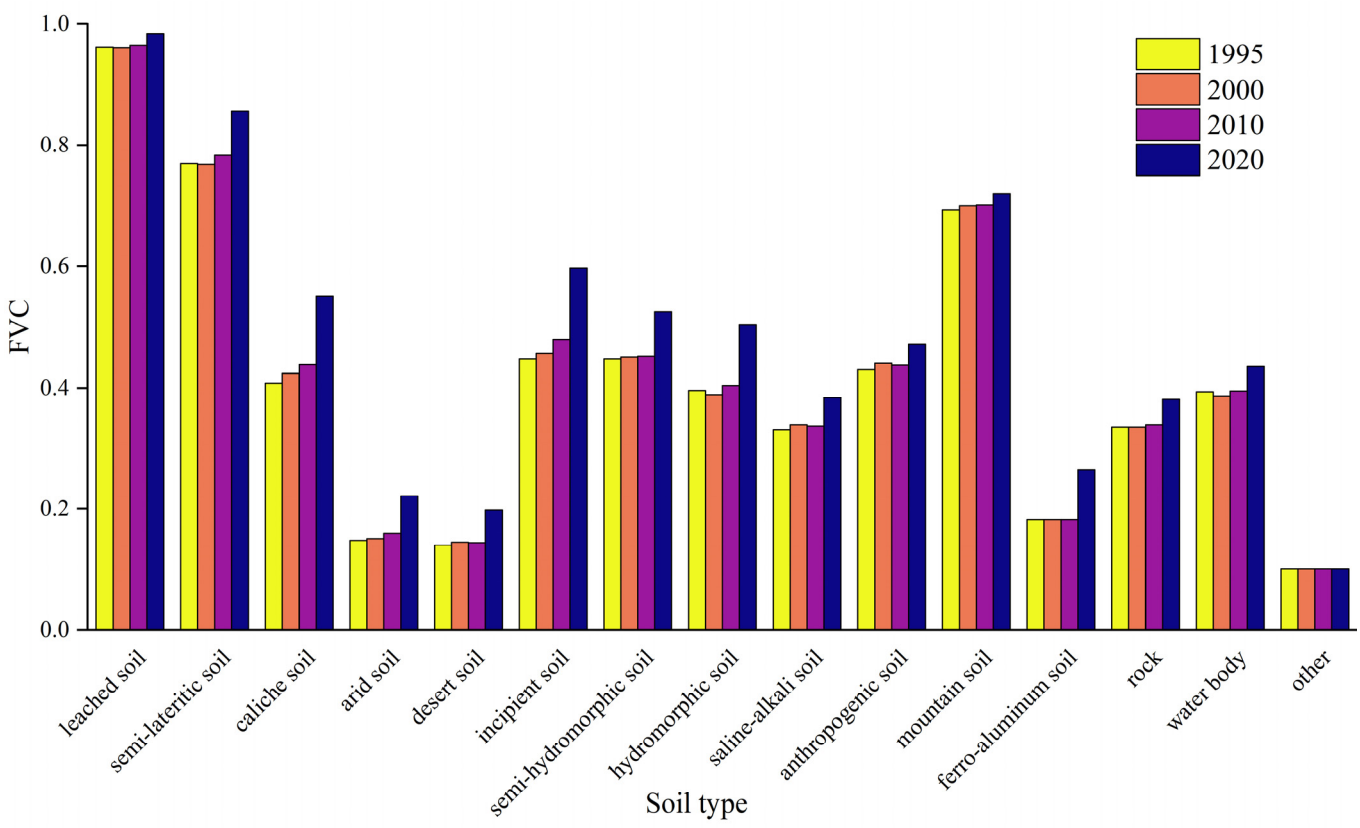

Figure 10. Average FVC under different soil types in 1995, 2000, 2010, and 2020.

Table 8. Percentage of area occupied by each land use type.

Zone Code	Land Use Type	FVC			
		1995	2000	2010	2020
1	cultivated land	0.533	0.543	0.564	0.663
2	forest land	0.933	0.929	0.935	0.963
3	grassland	0.366	0.371	0.382	0.486
4	water body	0.224	0.211	0.231	0.271
5	construction land	0.487	0.474	0.476	0.535
6	unused land	0.126	0.116	0.109	0.122

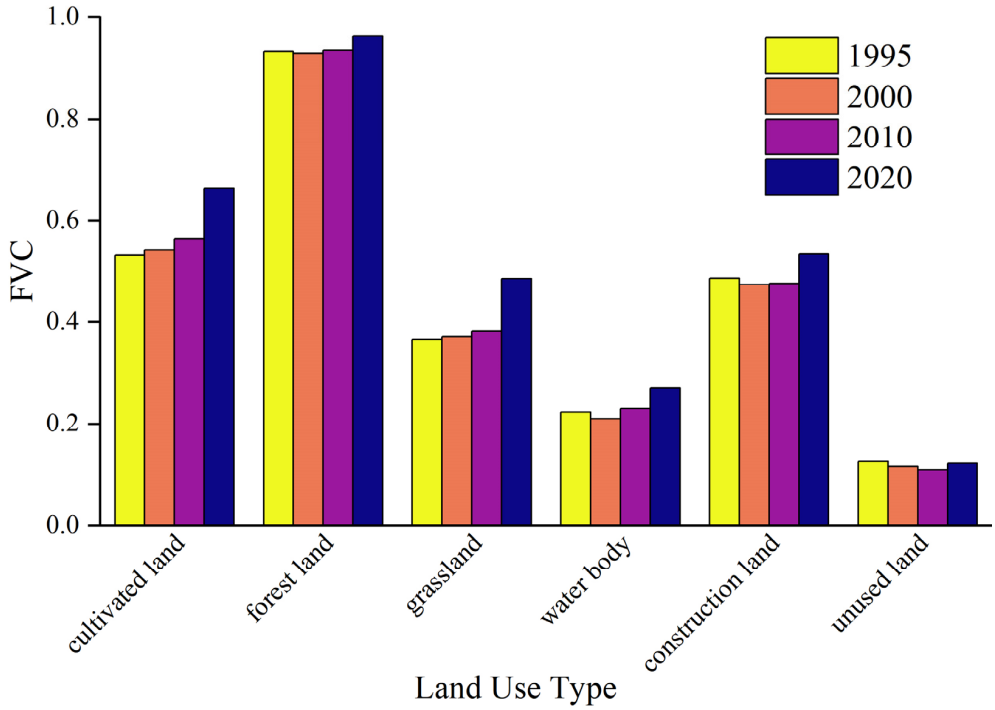

Figure 11. Average FVC under different land use types in 1995, 2000, 2010, and 2020.

3.2.3. Interaction Detection

To examine the changes in vegetation cover influenced by the interaction between natural and human factors, an interaction detector was employed to analyze the interactions of nine factors in 1995, 2000, 2010, and 2020. The explanatory power of the interaction among various driving factors is shown in Figure 12; the q-value matrix in the figure is symmetric about the diagonal, which represents the explanatory power of each factor on the vegetation cover change. The results indicate that in 1995, the q value of the interaction between land use and temperature and precipitation was the highest, at 0.65, making it the most prominent influence among the three factors during that study period. In 2000, 2010, and 2020, the two factors with the highest influence on vegetation cover under interaction were land use and precipitation, with q values of 0.79, 0.80, and 0.80, respectively. At all four time points, the interaction between precipitation and land use type has the greatest impact, indicating that precipitation and land use type are the most influential natural and human factors, respectively, affecting vegetation cover changes in the study area. Observing Figure 12a–d, it can be seen that the interaction impact of any factor with other factors is greater than the impact of the factor alone, demonstrating that the interactions among the nine selected factors in this study all exhibit mutual enhancement. Moreover, for any given factor, the greater the influence of the interacting factor, the stronger the interaction impact.

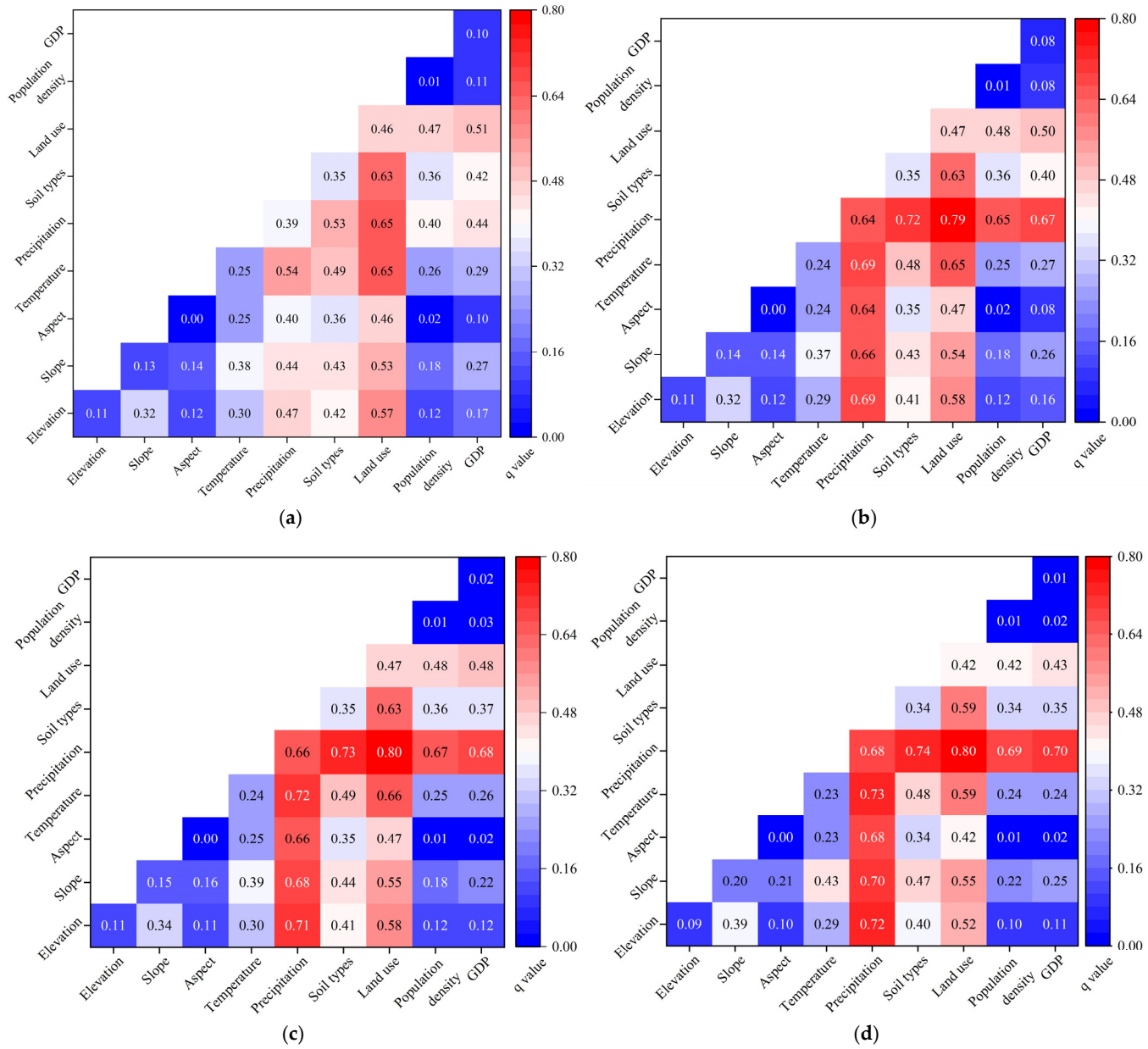

Figure 12. *q* value for detection of interaction effects of various factors in 1995, 2000, 2010, and 2020: (**a**) 1995; (**b**) 2000; (**c**) 2010; (**d**) 2020.

The analysis of the interaction between various factors affecting the spatial differentiation of vegetation cover (Table 9) reveals that, over the study period, the interactions among factors fell into two categories: nonlinear enhancement and dual-factor enhancement. Most of the factor interactions exhibit a two-factor enhancement, while a small portion show nonlinear enhancement, with the slope aspect factor interacting nonlinearly with other factors. Compared to 1995, 2000, and 2010, the factor interactions in 2020 show a notable increase in nonlinear enhancement.

Table 9. Interaction results of various factors in 1995, 2000, 2010, and 2020.

Interaction Factors	Interaction Results			
	1995	**2000**	**2010**	**2020**
Elevation ∩ Slope	↑↑	↑↑	↑↑	↑↑
Elevation ∩ Aspect	↑↑	↑↑	↑↑	↑↑
Elevation ∩ Temperature	↑	↑	↑	↑
Elevation ∩ Precipitation	↑	↑	↑	↑
Elevation ∩ Soil types	↑	↑	↑	↑
Elevation ∩ Land use	↑	↑	↑	↑↑
Elevation ∩ Population density	↑	↑	↑	↑↑
Elevation ∩ GDP	↑	↑	↑	↑
Slope ∩ Aspect	↑↑	↑↑	↑↑	↑↑
Slope ∩ Temperature	↑	↑	↑	↑↑
Slope ∩ Precipitation	↑	↑	↑	↑
Slope ∩ Soil types	↑	↑	↑	↑
Slope ∩ Land use	↑	↑	↑	↑
Slope ∩ Population density	↑↑	↑↑	↑↑	↑↑
Slope ∩ GDP	↑↑	↑↑	↑↑	↑↑
Aspect ∩ Temperature	↑↑	↑↑	↑↑	↑↑
Aspect ∩ Precipitation	↑↑	↑↑	↑↑	↑↑
Aspect ∩ Soil types	↑↑	↑↑	↑↑	↑↑
Aspect ∩ Land use	↑↑	↑↑	↑↑	↑↑
Aspect ∩ Population density	↑↑	↑↑	↑↑	↑↑
Aspect ∩ GDP	↑↑	↑↑	↑↑	↑↑
Temperature ∩ Precipitation	↑	↑	↑	↑
Temperature ∩ Soil types	↑	↑	↑	↑
Temperature ∩ Land use	↑	↑	↑	↑
Temperature ∩ Population density	↑	↑	↑	↑↑
Temperature ∩ GDP	↑	↑	↑	↑↑
Precipitation ∩ Soil types	↑	↑	↑	↑
Precipitation ∩ Land use	↑	↑	↑	↑
Precipitation ∩ Population density	↑	↑	↑	↑↑
Precipitation ∩ GDP	↑	↑	↑↑	↑↑
Soil types ∩ Land use	↑	↑	↑	↑
Soil types ∩ Population density	↑	↑	↑	↑↑
Soil types ∩ GDP	↑	↑	↑	↑
Land use ∩ Population density	↑	↑	↑	↑
Land use ∩ GDP	↑	↑	↑	↑↑
Population density ∩ GDP	↑	↑	↑	↑

Note: "↑" represents dual-factor enhancement, "↑↑" represents nonlinear enhancement.

Taking temperature, precipitation, soil type, and land use—four factors that significantly influence vegetation coverage—as examples, the average vegetation coverage under different driving factor ranges is analyzed and discussed. The suitable ranges for each driving factor are shown in Table 10. In 1995, 2000, 2010, and 2020, the suitable ranges for land use and soil type remained consistent, with the highest average FVC values found in areas where the land use type was forest land and the soil type was leaching soil. Due to the significant differences in the precipitation and temperature data across different years, the suitable ranges for precipitation and temperature are related to their respective annual data partitions. The results show that on the Loess Plateau, the highest average FVC values occur when precipitation ranges from 630.64 to 935.51 mm and temperatures range from −4.38 to 2 °C. However, considering that temperatures on the Loess Plateau are gradually rising and the FVC showed an upward trend during the second peak in 2020, the optimal temperature for vegetation on the Loess Plateau in the future may exceed 16 °C. When vegetation is within the optimal growth range for each factor, the average vegetation coverage will significantly increase. However, existing studies have shown that there is an upper limit to vegetation coverage, with the vegetation coverage threshold being 65% [47].

Table 10. The suitable range and types of vegetation coverage in 1995, 2000, 2010, and 2020.

Factors	Suitable Types or Ranges			
	1995	**2000**	**2010**	**2020**
Temperature	−1.75–1.02	−1.42–1.49	−1.05–1.87	−4.38–2.00
Precipitation	733.72–931.58	630.64–802.62	698.83–880.68	752.01–935.51
Soil types	Leached soil	Leached soil	Leached soil	Leached soil
Land use	Forest land	Forest land	Forest land	Forest land

4. Discussion

4.1. Factor Interaction Effects

The changes in the vegetation coverage on the Loess Plateau are influenced by multiple factors. This study examines the influence of various natural and human-induced factors on vegetation coverage. The population density reflects the number of people in the area; generally, population growth tends to encroach on ecological land, leading to a decrease in the vegetation coverage. Related studies have shown that a reduction in the vegetation coverage is closely related to a high population growth rate [48]. Some scholars have pointed out that the widely held belief of an inverse relationship between population growth and vegetation coverage may not hold true [49]. Their research suggests that in regions where human activities are frequent and climate change has minimal influence on vegetation coverage, a long-term inverted N-shaped relationship exists between population growth and vegetation coverage. Initially, population growth negatively affects vegetation coverage, but over time, it begins to have a positive impact.

The GDP represents the area's level of economic development. Some scholars believe that excessively rapid economic development can adversely affect the local natural environment [50]. However, other scholars argue that effective policies can achieve both rapid economic growth and increased vegetation coverage [51]. Since the conclusion of the last century, various measures, including returning farmland to forest and afforestation, have been carried out in the Loess Plateau region to mitigate soil loss and enhance the ecological environment.

Some researchers believe that vegetation conditions largely depend on the current land use status. Different land use types can be categorized into specific vegetation units, and changes in land use result in alterations to vegetation characteristics, establishing it as one of the key drivers of vegetation change [52]. This study also demonstrates that land use type is among the most influential factors impacting vegetation coverage, and the maximum interactive impact occurs when precipitation interacts with the land use type in different time periods.

Precipitation, as an essential factor in the vegetation growth process, is the most significant factor influencing the vegetation coverage in the findings of this study. Research indicates a significant positive correlation between vegetation and precipitation in semi-arid to semi-humid regions [53], with plant growth being especially responsive to precipitation anomalies. Some scholars have also found correlations between precipitation and vegetation coverage in arid and semi-arid regions [54]. The average annual precipitation in the Loess Plateau ranges from 100 mm to 700 mm, with most areas being arid, semi-arid, or semi-humid. According to the research findings, there is a significant correlation between vegetation coverage and precipitation in the Loess Plateau region. Scholars have noted that vegetation coverage on the Chinese mainland is strongly correlated with both precipitation and temperature, with a more pronounced correlation with temperature [55]. Research has indicated that at an interannual scale, precipitation is the primary driver of vegetation coverage in the entire region, and at an inter-monthly scale, changes in the vegetation coverage align with changes in precipitation and temperature [56]. This suggests that

the responsiveness of vegetation growth to the combined influences of water and heat throughout the year exceeds that of any single climatic factor. In this study, it is shown that the interactive effects of precipitation and temperature are greater than those of each factor independently.

The soil types in this study were categorized into 15 classes, and the results indicated that leaching soil is the most conducive for vegetation growth. Related research has demonstrated that in areas with low precipitation, soil moisture is positively correlated with vegetation, and this correlation decreases as one moves from arid to semi-arid or semi-humid regions [57]. Different soil types possess distinct physical and chemical characteristics, leading to differences in the soil moisture content and thus affecting vegetation growth differently. Although the slope orientation has a relatively small direct effect on vegetation, its interactions with other natural and anthropogenic factors can produce significant impacts. Relevant studies indicate that soil moisture effectiveness is associated with topography, which subsequently impacts vegetation growth [58]. For example, north-facing slopes receive less solar radiation and experience lower evaporation rates compared to south-facing slopes, leading to a relatively higher soil moisture that is more conducive to vegetation growth. Within a specific range, the steeper the slope, the greater the difference in the soil moisture between north and south slopes, and the slope also influences land use types to some extent, affecting vegetation. In the same area, a certain elevation difference can lead to varying temperatures and precipitation levels; therefore, elevation affects vegetation coverage by influencing climatic factors.

4.2. Study Limitations and Uncertainties

This study has certain limitations and uncertainties. For instance, this study did not use 30 m resolution Landsat data but instead employed the coarser-resolution MODIS data. The reason for this is that higher-spatial-resolution data have a larger data volume, which would require an excessively large workload for long-term trend studies. However, this means that the obtained vegetation coverage represents an average value over a larger area. This may introduce uncertainties in the quantitative analysis of the spatiotemporal changes in vegetation coverage. In future studies, higher-resolution Landsat data could be considered for calculating the FVC, along with other higher-resolution factor data. This would enhance the accuracy of the results. Additionally, the Geodetector model requires data discretization, such as land use classification and precipitation grading. Different classification or grading standards may yield varying results. Therefore, multiple experiments are needed to comprehensively compare different classification or grading methods and ultimately determine the optimal standard.

5. Conclusions

This study uses the NDVI dataset as a data source to assess and calculate vegetation coverage, investigating the spatiotemporal changes in vegetation coverage on the Loess Plateau from 1995 to 2020. By integrating data on land use types, temperature, precipitation, slope, and other factors, the geographical detector model was employed to evaluate the impact of these factors on vegetation coverage changes on the Loess Plateau and to analyze the driving mechanisms behind these changes in vegetation coverage. The following conclusions were drawn:

(1) From a temporal perspective, the average annual vegetation coverage on the Loess Plateau increased from 0.36 in 1995 to 0.6 in 2020, with minor fluctuations but an overall monotonic upward trend at a growth rate of 0.01021 per year. Spatially, most areas of the Loess Plateau exhibited a significantly increasing trend in vegetation

coverage, a small portion showed no significant changes, and a very small portion experienced a significantly decreasing trend.

(2) Among natural factors, the influence of the altitude, slope, and aspect is relatively minor, while the temperature, precipitation, and soil type have a greater impact, with precipitation being the most significant factor affecting changes in vegetation cover. Among human factors, land use has the greatest influence on vegetation growth, while the population density and GDP have a relatively smaller impact on the spatial variation in vegetation cover. Furthermore, the interactive effects of various factors on vegetation cover change exceed their individual effects, exhibiting characteristics of mutual enhancement and nonlinear amplification.

(3) According to the results from the geographical detector model, the highest average vegetation coverage is achieved when the temperature is between −4.8 and 2 °C or 12 and 16 °C, precipitation is between 630.64 and 935.51 mm, the soil type is leaching soil, and the land use type is forest. Under these conditions, the vegetation growth status is at its best.

The changes in vegetation cover on the Loess Plateau are influenced by multiple factors. Some of the factors selected in this study have relatively minor impacts. In future research on vegetation cover changes in other regions, less influential factors should be excluded, and unconsidered factors should be included. This approach aims to scientifically analyze and reveal the effects of different driving factors on vegetation cover changes as comprehensively as possible, thereby effectively guiding vegetation restoration and conservation in the study area.

Author Contributions: Conceptualization, Z.Y. and Q.Y.; methodology, Z.Y.; software, Y.Z.; validation, Y.Z. and Y.H.; formal analysis, Q.Y.; investigation, Y.Z.; resources, Z.Y.; data curation, Y.Z.; writing—original draft preparation, Y.H.; writing—review and editing, Y.H., M.Y., Q.Y. and Z.Y.; visualization, Y.H.; supervision, Z.Y. and P.J.; project administration, Q.Y.; funding acquisition, Q.Y., P.J. and M.Y. All authors have read and agreed to the published version of the manuscript.

Funding: This research was funded by the National Natural Science Foundation of China, grant numbers U2243210 and 42401384, the National Key Research and Development Program, grant number 2022YFF130080101, the Science and Technology Development of Henan Province of China, grant number 242102320252, the Inner Mongolia Autonomous Region "Top Talent Leadership Recruitment" Project, grant number 150000243033210000057, and Humanity and Social Science Foundation of Ministry of Education, grant number 24YJCZH376.

Data Availability Statement: No new data were created or analyzed in this study. Data sharing is not applicable to this article.

Conflicts of Interest: The authors declare no conflicts of interest.

References

1. Song, W.; Mu, X.; Ruan, G.; Gao, Z.; Li, L.; Yan, G. Estimating fractional vegetation cover and the vegetation index of bare soil and highly dense vegetation with a physically based method. *Int. J. Appl. Earth Obs. Geoinf.* **2017**, *58*, 168–176. [CrossRef]
2. Dong, L.; Li, J.; Zhang, Y.; Bing, M.; Liu, Y.; Wu, J.; Hai, X.; Li, A.; Wang, K.; Wu, P. Effects of vegetation restoration types on soil nutrients and soil erodibility regulated by slope positions on the Loess Plateau. *J. Environ. Manag.* **2022**, *302*, 113985. [CrossRef]
3. Zhou, J.; Fu, B.; Gao, G.; Lü, Y.; Liu, Y.; Lü, N.; Wang, S. Effects of precipitation and restoration vegetation on soil erosion in a semi-arid environment in the Loess Plateau, China. *Catena* **2016**, *137*, 1–11. [CrossRef]
4. Gao, L.; Wang, X.; Johnson, B.A.; Tian, Q.; Wang, Y.; Verrelst, J.; Mu, X.; Gu, X. Remote sensing algorithms for estimation of fractional vegetation cover using pure vegetation index values: A review. *ISPRS J. Photogramm. Remote Sens.* **2020**, *159*, 364–377. [CrossRef]
5. Liu, Q.; Zhang, T.; Li, Y.; Li, Y.; Bu, C.; Zhang, Q. Comparative analysis of fractional vegetation cover estimation based on multi-sensor data in a semi-arid sandy area. *Chin. Geogr. Sci.* **2019**, *29*, 166–180. [CrossRef]

6. Yang, P.; Tian, J.; Zhang, N.; Gao, Y.; Feng, X.; Yang, C.; Peng, D. Characteristics of spatio-temporal changes and future trends forecast of vegetation cover in the Yellow River Basin from 1990 to 2022. *Acta Ecol. Sin.* **2024**, *44*, 1–12.
7. Liu, Y.; Feng, Y.; Zhao, Z.; Zhang, Q.; Su, S. Socioeconomic drivers of forest loss and fragmentation: A comparison between different land use planning schemes and policy implications. *Land Use Policy* **2016**, *54*, 58–68. [CrossRef]
8. Johnson, B.; Tateishi, R.; Kobayashi, T. Remote sensing of fractional green vegetation cover using spatially-interpolated endmembers. *Remote Sens.* **2012**, *4*, 2619–2634. [CrossRef]
9. Cao, Q.; Yu, D.; Georgescu, M.; Han, Z.; Wu, J. Impacts of land use and land cover change on regional climate: A case study in the agro-pastoral transitional zone of China. *Environ. Res. Lett.* **2015**, *10*, 124025. [CrossRef]
10. Pettorelli, N. *The Normalized Difference Vegetation Index*; Oxford University Press: Cary, NC, USA, 2013.
11. Wu, D.; Wu, H.; Zhao, X.; Zhou, T.; Tang, B.; Zhao, W.; Jia, K. Evaluation of spatiotemporal variations of global fractional vegetation cover based on GIMMS NDVI data from 1982 to 2011. *Remote Sens.* **2014**, *6*, 4217–4239. [CrossRef]
12. Vicente-Serrano, S.M.; Camarero, J.J.; Olano, J.M.; Martín-Hernández, N.; Peña-Gallardo, M.; Tomás-Burguera, M.; Gazol, A.; Azorin-Molina, C.; Bhuyan, U.; El Kenawy, A. Diverse relationships between forest growth and the Normalized Difference Vegetation Index at a global scale. *Remote Sens. Environ.* **2016**, *187*, 14–29. [CrossRef]
13. Li, F.; Chen, W.; Zeng, Y.; Zhao, Q.; Wu, B. Improving estimates of grassland fractional vegetation cover based on a pixel dichotomy model: A case study in Inner Mongolia, China. *Remote Sens.* **2014**, *6*, 4705–4722. [CrossRef]
14. Liu, G.; Shangguan, Z.; Yao, W.; Yang, Q.; Zhao, M.; Dang, X.; Guo, M.; Wang, G.; Wang, B. Ecological effects of soil conservation in Loess Plateau. *Bull. Chin. Acad. Sci. (Chin. Version)* **2017**, *32*, 11–19.
15. Jiapaer, G.; Chen, X.; Bao, A. A comparison of methods for estimating fractional vegetation cover in arid regions. *Agric. For. Meteorol.* **2011**, *151*, 1698–1710. [CrossRef]
16. Zhang, X.; Liao, C.; Li, J.; Sun, Q. Fractional vegetation cover estimation in arid and semi-arid environments using HJ-1 satellite hyperspectral data. *Int. J. Appl. Earth Obs. Geoinf.* **2013**, *21*, 506–512. [CrossRef]
17. Wang, G.; Wang, J.; Zou, X.; Chai, G.; Wu, M.; Wang, Z. Estimating the fractional cover of photosynthetic vegetation, non-photosynthetic vegetation and bare soil from MODIS data: Assessing the applicability of the NDVI-DFI model in the typical Xilingol grasslands. *Int. J. Appl. Earth Obs. Geoinf.* **2019**, *76*, 154–166. [CrossRef]
18. Li, T.; Li, X.S.; Li, F. Estimating fractional cover of photosynthetic vegetation and non—Photosynthetic vegetation in the Xilingol steppe region with EO-1 hyperion data. *Acta Ecol. Sin.* **2015**, *35*, 3643–3652.
19. Cong, N.; Shen, M.; Yang, W.; Yang, Z.; Zhang, G.; Piao, S. Varying responses of vegetation activity to climate changes on the Tibetan Plateau grassland. *Int. J. Biometeorol.* **2017**, *61*, 1433–1444. [CrossRef]
20. Sun, C.; Liu, Y.; Song, H.; Li, Q.; Cai, Q.; Wang, L.; Fang, C.; Liu, R. Tree-ring evidence of the impacts of climate change and agricultural cultivation on vegetation coverage in the upper reaches of the Weihe River, northwest China. *Sci. Total Environ.* **2020**, *707*, 136160. [CrossRef]
21. Rodrigues, P.M.S.; Schaefer, C.E.G.R.; de Oliveira Silva, J.; Ferreira Júnior, W.G.; dos Santos, R.M.; Neri, A.V. The influence of soil on vegetation structure and plant diversity in different tropical savannic and forest habitats. *J. Plant Ecol.* **2018**, *11*, 226–236. [CrossRef]
22. Sato, H.; Kobayashi, H.; Beer, C.; Fedorov, A. Simulating interactions between topography, permafrost, and vegetation in Siberian larch forest. *Environ. Res. Lett.* **2020**, *15*, 095006. [CrossRef]
23. Wang, R.; Yan, F.; Wang, Y. Vegetation growth status and topographic effects in the pisha sandstone area of China. *Remote Sens.* **2020**, *12*, 2759. [CrossRef]
24. Hua, W.; Chen, H.; Zhou, L.; Xie, Z.; Qin, M.; Li, X.; Ma, H.; Huang, Q.; Sun, S. Observational quantification of climatic and human influences on vegetation greening in China. *Remote Sens.* **2017**, *9*, 425. [CrossRef]
25. Piao, S.; Wang, X.; Park, T.; Chen, C.; Lian, X.; He, Y.; Bjerke, J.W.; Chen, A.; Ciais, P.; Tømmervik, H. Characteristics, drivers and feedbacks of global greening. *Nat. Rev. Earth Environ.* **2020**, *1*, 14–27. [CrossRef]
26. Xiong, J.; Peng, C.; Cheng, W.; Li, W.; Liu, Z.Q.; Fan, C.K.; Sun, H.Z. Analysis of Vegetation Coverage Change in Yunnan Province Based on MODIS-NDVI. *J. Geo-Inf. Sci.* **2018**, *20*, 1830–1840.
27. Shi, P.; Hou, P.; Gao, J.; Wan, H.; Wang, Y.; Sun, C. Spatial-temporal variation characteristics and influencing factors of vegetation in the Yellow River Basin from 2000 to 2019. *Atmosphere* **2021**, *12*, 1576. [CrossRef]
28. Ma, H.X.; Chen, C.C.; Song, Y.Q.; Ye, S.; Hu, Y.M. Analysis of Vegetation Cover Change and Its Driving Factors over the Past Ten Years in Qinghai Province. *Res. Soil Water Conserv.* **2018**, *25*, 137–145.
29. Zhang, C.S.; Hu, Y.; Shi, X.L. Analysis of Spatial-Temporal Evolution of Vegetation Cover in Loess Plateau in Recent 33 Years Based on AVHRR NDVI and MODIS NDVI. *J. Appl. Sci.* **2016**, *34*, 702–712.
30. Wang, J.F.; Li, X.H.; Christakos, G.; Liao, Y.L.; Zhang, T.; Gu, X.; Zheng, X.Y. Geographical detectors-based health risk assessment and its application in the neural tube defects study of the Heshun Region, China. *Int. J. Geogr. Inf. Sci.* **2010**, *24*, 107–127. [CrossRef]
31. Wang, J.; Xu, C. Geodetector: Principle and prospective. *Acta Ecol. Sin.* **2017**, *72*, 116–134. [CrossRef]

32. Peng, W.; Kuang, T.; Tao, S. Quantifying influences of natural factors on vegetation NDVI changes based on geographical detector in Sichuan, western China. *J. Clean. Prod.* **2019**, *233*, 353–367. [CrossRef]
33. Wang, G.; Peng, W. Quantifying spatiotemporal dynamics of vegetation and its differentiation mechanism based on geographical detector. *Environ. Sci. Pollut. Res.* **2022**, *29*, 32016–32031. [CrossRef]
34. Li, M.; Han, Y.; Zhao, H.; Wang, Y. Analysis on spatial-temporal variation characteristics and driving factors of fractional vegetation cover in Ningxia based on geographical detector. *Ecol. Environ.* **2022**, *31*, 1317.
35. Liang, P.; Yang, X. Landscape spatial patterns in the Maowusu (Mu Us) Sandy Land, northern China and their impact factors. *Catena* **2016**, *145*, 321–333. [CrossRef]
36. Wang, J.-F.; Hu, Y. Environmental health risk detection with GeogDetector. *Environ. Model. Softw.* **2012**, *33*, 114–115. [CrossRef]
37. Li, P.; Mu, X.; Holden, J.; Wu, Y.; Irvine, B.; Wang, F.; Gao, P.; Zhao, G.; Sun, W. Comparison of soil erosion models used to study the Chinese Loess Plateau. *Earth-Sci. Rev.* **2017**, *170*, 17–30. [CrossRef]
38. Wen, X.; Zhen, L. Soil erosion control practices in the Chinese Loess Plateau: A systematic review. *Environ. Dev.* **2020**, *34*, 100493. [CrossRef]
39. Yu, Z.; Deng, X.; Cheshmehzangi, A. The grain for green program enhanced synergies between ecosystem regulating services in Loess Plateau, China. *Remote Sens.* **2022**, *14*, 5940. [CrossRef]
40. Tian, L.; Zhang, B.; Wang, X.; Chen, S.; Pan, B. Large-scale afforestation over the Loess Plateau in China contributes to the local warming trend. *J. Geophys. Res. Atmos.* **2022**, *127*, e2021JD035730. [CrossRef]
41. Peng, S. *1-km Monthly Mean Temperature Dataset for China (1901–2022)*; National Tibetan Plateau Data Center: Beijing, China, 2019.
42. Peng, S. *1-km Monthly Precipitation Dataset for China (1901–2020)*; National Tibetan Plateau Data Center: Beijing, China, 2020.
43. Yang, J.; Huang, X. 30 m annual land cover and its dynamics in China from 1990 to 2019. *Earth Syst. Sci. Data Discuss.* **2021**, *2021*, 1–29.
44. Chen, B.-M.; Zhou, X.-P. Explanation of Current Land Use Condition Classification for National Standard of the People's Republic of China. *J. Nat. Resour.* **2007**, *22*, 994–1003.
45. Behdani, Z.; Darehmiraki, M. Theil-Sen Estimators for fuzzy regression model. *Iran. J. Fuzzy Syst.* **2024**, *21*, 177–192.
46. Yuan, L.; Jiang, W.; Shen, W.; Liu, Y.; Wang, W.; Tao, L.; Zheng, H.; Liu, X. The spatio-temporal variations of vegetation cover in the Yellow River Basin from 2000 to 2010. *Acta Ecol. Sin.* **2013**, *33*, 7798–7806. [CrossRef]
47. Chen, Y.-P.; Wang, K.-B.; Fu, B.-J.; Wang, Y.-F.; Tian, H.-W.; Wang, Y.; Zhang, Y. 65% cover is the sustainable vegetation threshold on the Loess Plateau. *Environ. Sci. Ecotechnology* **2024**, *22*, 100442. [CrossRef]
48. Brandt, M.; Rasmussen, K.; Peñuelas, J.; Tian, F.; Schurgers, G.; Verger, A.; Mertz, O.; Palmer, J.R.; Fensholt, R. Human population growth offsets climate-driven increase in woody vegetation in sub-Saharan Africa. *Nat. Ecol. Evol.* **2017**, *1*, 0081. [CrossRef]
49. Liu, C.; Xie, W.; Lao, T.; Yao, Y.-t.; Zhang, J. Application of a novel grey forecasting model with time power term to predict China's GDP. *Grey Syst. Theory Appl.* **2021**, *11*, 343–357. [CrossRef]
50. Hu, M.; Xia, B. A significant increase in the normalized difference vegetation index during the rapid economic development in the Pearl River Delta of China. *Land Degrad. Dev.* **2019**, *30*, 359–370. [CrossRef]
51. Li, C.; Kuang, Y.; Huang, N.; Zhang, C. The long-term relationship between population growth and vegetation cover: An empirical analysis based on the panel data of 21 cities in Guangdong province, China. *Int. J. Environ. Res. Public Health* **2013**, *10*, 660–677. [CrossRef]
52. Tasser, E.; Tappeiner, U. Impact of land use changes on mountain vegetation. *Appl. Veg. Sci.* **2002**, *5*, 173–184. [CrossRef]
53. Jiang, D.; Zhang, H.; Zhang, Y.; Wang, K. Interannual variability and correlation of vegetation cover and precipitation in Eastern China. *Theor. Appl. Climatol.* **2014**, *118*, 93–105. [CrossRef]
54. Mo, K.; Chen, Q.; Chen, C.; Zhang, J.; Wang, L.; Bao, Z. Spatiotemporal variation of correlation between vegetation cover and precipitation in an arid mountain-oasis river basin in northwest China. *J. Hydrol.* **2019**, *574*, 138–147. [CrossRef]
55. Chen, H.; Ren, Z. Response of vegetation coverage to changes of precipitation and temperature in Chinese mainland. *Bull. Soil Water Conserv* **2013**, *2*, 18.
56. Mu, S.; Yang, H.; Li, J.; Chen, Y.; Gang, C.; Zhou, W.; Ju, W. Spatio-temporal dynamics of vegetation coverage and its relationship with climate factors in Inner Mongolia, China. *J. Geogr. Sci.* **2013**, *23*, 231–246. [CrossRef]
57. D'Odorico, P.; Caylor, K.; Okin, G.S.; Scanlon, T.M. On soil moisture–vegetation feedbacks and their possible effects on the dynamics of dryland ecosystems. *J. Geophys. Res. Biogeosci.* **2007**, *112*. [CrossRef]
58. Fan, J.; Xu, Y.; Ge, H.; Yang, W. Vegetation growth variation in relation to topography in Horqin Sandy Land. *Ecol. Indic.* **2020**, *113*, 106215. [CrossRef]